Identification of the 2-Hydroxyglutarate and Isovaleryl-CoA Dehydrogenases as Alternative Electron Donors Linking Lysine Catabolism to the Electron Transport Chain of *Arabidopsis* Mitochondria [W][OA]

Wagner L. Araújo,[a,1] Kimitsune Ishizaki,[b,1] Adriano Nunes-Nesi,[a] Tony R. Larson,[c] Takayuki Tohge,[a] Ina Krahnert,[a] Sandra Witt,[a] Toshihiro Obata,[a] Nicolas Schauer,[a,2] Ian A. Graham,[c] Christopher J. Leaver,[d] and Alisdair R. Fernie[a,3]

[a] Max Planck Institut für Molekulare Pflanzenphysiologie, 14476 Golm, Germany
[b] Graduate School of Biostudies, Kyoto University, Kyoto 606-8502, Japan
[c] Department of Biology, Centre for Novel Agricultural Products, University of York, Heslington, York YO10 5YW, United Kingdom
[d] Department of Plant Sciences, University of Oxford, Oxford OX1 3RB, United Kingdom

The process of dark-induced senescence in plants is relatively poorly understood, but a functional electron-transfer flavoprotein/electron-transfer flavoprotein:ubiquinone oxidoreductase (ETF/ETFQO) complex, which supports respiration during carbon starvation, has recently been identified. Here, we studied the responses of *Arabidopsis thaliana* mutants deficient in the expression of isovaleryl-CoA dehydrogenase and 2-hydroxyglutarate dehydrogenase to extended darkness and other environmental stresses. Evaluations of the mutant phenotypes following carbon starvation induced by extended darkness identify similarities to those exhibited by mutants of the ETF/ETFQO complex. Metabolic profiling and isotope tracer experimentation revealed that isovaleryl-CoA dehydrogenase is involved in degradation of the branched-chain amino acids, phytol, and Lys, while 2-hydroxyglutarate dehydrogenase is involved exclusively in Lys degradation. These results suggest that isovaleryl-CoA dehydrogenase is the more critical for alternative respiration and that a series of enzymes, including 2-hydroxyglutarate dehydrogenase, plays a role in Lys degradation. Both physiological and metabolic phenotypes of the isovaleryl-CoA dehydrogenase and 2-hydroxyglutarate dehydrogenase mutants were not as severe as those observed for mutants of the ETF/ETFQO complex, indicating some functional redundancy of the enzymes within the process. Our results aid in the elucidation of the pathway of plant Lys catabolism and demonstrate that both isovaleryl-CoA dehydrogenase and 2-hydroxyglutarate dehydrogenase act as electron donors to the ubiquinol pool via an ETF/ETFQO-mediated route.

INTRODUCTION

In mammals, the nuclear-encoded mitochondrial protein, electron-transfer flavoprotein:ubiquinone oxidoreductase (ETFQO), which is associated with the inner mitochondrial membrane, accepts electrons from the electron-transfer flavoprotein (ETF) localized in the mitochondrial matrix and reduces ubiquinone (Ruzicka and Beinert, 1977; Beckmann and Frerman, 1985; Zhang et al., 2006). ETF is the physiological electron acceptor for at least nine mitochondrial matrix flavoprotein dehydrogenases. The ETF/ETFQO system can thus be thought of as a branch of the electron transport system with multiple input sites from seven acyl-CoA dehydrogenases and two N-methyl dehydrogenases, namely, isovaleryl-CoA dehydrogenase (IVDH) and 2-methyl branched-chain acyl-CoA dehydrogenase, as well as glutaryl-CoA dehydrogenase and sarcosine and dimethylglycine dehydrogenases (Frerman, 1988; Frerman and Goodman, 2001). While the ETF/ETFQO system has been extensively characterized in mammalian cells and mutations in it cause the fatal genetic disease Glutaric acidemia type II (multiple acyl-CoA dehydrogenase dysfunctional disease; Frerman and Goodman, 2001), it has only recently been characterized in plants.

In *Arabidopsis thaliana*, the ETF/ETFQO system was identified in mitochondria by the use of gel-based or liquid chromatography tandem mass spectrometry mitochondrial proteomic analysis (Heazlewood et al., 2004) and demonstrated to be induced at the level of transcription during dark-induced senescence (Buchanan-Wollaston et al., 2005) and oxidative stress (Lehmann et al., 2009). In addition, the functional role of both ETFQO and ETF itself was recently established via a characterization of allelic T-DNA mutants of the ETFQO protein and of the β-subunit of ETF (Ishizaki et al., 2005, 2006). The latter studies demonstrated

the formation of a similar complex in plants as those previously characterized in microbial and mammalian systems (Frerman, 1988; Frerman and Goodman, 2001; Swanson et al., 2008). Moreover, metabolic profiling of leaves from the wild type and all mutants following transfer to extended periods of darkness revealed a dramatic decline in sugar levels. In contrast with the wild type, all mutant lines demonstrated significant accumulation of several amino acids, an intermediate of Leu catabolism, and phytanoyl-CoA, a chlorophyll degradation product. These data demonstrate the involvement of the ETF/ETFQO system in the catabolism of branched-chain amino acids, as well as implying its involvement in the breakdown of other amino acids and chlorophyll during conditions of dark-induced senescence. These findings lead to an expansion of the number of dehydrogenases thought to be of direct importance for the functionality of the mitochondrial electron transport chain (Rasmusson et al., 2008). Recently, a plant 2-hydroxyglutarate dehydrogenase (D2HGDH) was characterized (Engqvist et al., 2009) and shown, as in animals (Achouri et al., 2004), to catalyze the degradation of 2-hydroxyglutarate to 2-oxoglutarate. Furthermore, T-DNA insertional knockouts of the single gene that encodes this enzyme were isolated and shown, in contrast with D-lactate dehydrogenase knockout mutants, to be insensitive to growth inhibition following growth on either D-lactate or methylglyoxal. Finally, on the basis of coexpression analysis and theoretical knowledge, the authors postulated that D2HGDH is responsible for supplying the ETF/ETFQO system with electrons following the degradation of both branched-chain amino acids and phytol (Engqvist et al., 2009).

Here, we demonstrate that breakdown of phytol and branched-chain amino acids to support electron provision to the ETF/ETFQO complex in plant mitochondria is predominantly catalyzed by IVDH, while D2HGDH is responsible for input to the complex solely via the degradation of Lys. These findings demonstrate that both enzymes play key, albeit conditional, roles in the maintenance of mitochondrial respiration but suggest that the IVDH is quantitatively more important, at least under conditions of prolonged darkness. While the links among IVDH, D2HGDH, and the ETF/ETFQO complex have been described in plants and other systems (Frerman, 1988; Frerman and Goodman, 2001; Ishizaki et al., 2005; Engqvist et al., 2009), this study indicates that Lys catabolism can directly channel electrons to the mitochondrial electron transport chain in addition to sustaining the operation of the tricarboxylic acid (TCA) cycle under C-limiting conditions.

RESULTS

Isolation of T-DNA Insertional Mutants of IVDH and D2HGDH

To investigate the in vivo functions of the IVDH and D2HGDH proteins, independent *Arabidopsis* lines were isolated that contained T-DNA elements inserted into the *IVDH* and *D2HGDH* genes. Segregation analysis of the encoded antibiotic resistance markers in the two insertional elements was in good agreement with the 3:1 (resistant:susceptible) ratio, suggesting insertion at a single Mendelian locus. Homozygous lines for each mutant were

characterized by genomic PCR and designated *ivdh-1* and *d2hgdh1-2*, respectively (Figure 1). The respective sites of insertion of these mutants were confirmed by sequencing of PCR products amplified from each mutant. RT-PCR using primer pairs designed to span the T-DNA insertion sites of the two mutant loci was used to investigate transcription of both *IVDH* and *D2HGDH*. The *Arabidopsis* β-tubulin gene, *TUB9*, was used as a control to demonstrate the integrity of the RNA preparation. *IVDH* and *D2HGDH* mRNAs were detected in the wild type (Columbia-0 [Col-0]) using the primer set L1/R1 and L2/R2, respectively; however, no amplification products were observed for the transcripts in *ivdh-1* and *d2hgdh1-2* (Figure 1). Thus, these results confirm that transcripts spanning the T-DNA insertion site are absent in these mutant lines.

Phenotypes of *ivdh-1* and *d2hgdh1-2* Lines

Following the characterization of the molecular identity of the T-DNA insertional mutants, they were grown in soil under long-day (16 h light/8 h dark) conditions alongside wild-type controls. Under these conditions, there were no visible aberrant phenotypes in the mutants during vegetative growth. When 4-week-old
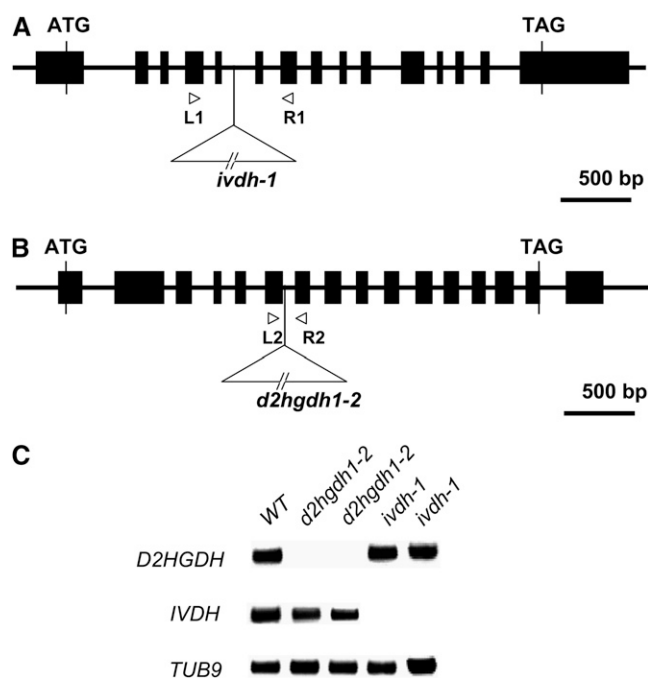

Figure 1. A Schematic Representation of the Sites of T-DNA Insertion in the Mutants.

(A) and **(B)** Genomic structure of *IVDH* **(A)** and *D2HGDH* **(B)**. Arrowheads represent positions of primers used for genotyping of wild-type and mutant lines; closed boxes indicate exons. In *ivdh-1*, the T-DNA is inserted in intron 5 of *IVDH*. In *d2hgdh1-2*, the T-DNA is inserted in intron 6 of *D2HGDH*.

(C) RT-PCR analysis on total RNA from the wild type (WT) and the *d2hgdh1-2* and *ivdh-1* mutant lines, with primer sets for the genes indicated on the left. The positions of the primers in the *IVDH* and *D2HGDH* genomic loci are represented in **(A)** and **(B)**, respectively.

ivdh-1 and *d2hgdh1-2* mutants grown under short-day (8 h light/ 16 h dark) conditions were transferred to extended dark conditions alongside the previously characterized *etfqo* mutants (Ishizaki et al., 2005), a range of phenotypes became apparent. All of the homozygous mutant lines started to wilt and show signs of senescence after 10 d of continuous darkness, and the *etfqo-1* and *etfqo-2* mutants were apparently dead after 15 d of continuous darkness, whereas wild-type and, more importantly, complemented mutant plants were still alive and exhibited only limited signs of senescence and no visible abnormalities (Figure 2A). It is noteworthy that *d2hgdh1-2* and *ivdh-1* also showed strong signs of senescence but with a less severe phenotype compared with wild-type plants than *etfqo* plants displayed (Figure 2A). To investigate further this apparent accelerated

senescence in all mutants, we measured two parameters related to the function of chloroplasts, chlorophyll content and photochemical efficiency (maximum variable fluorescence/ maximum yield of fluorescence [F_v/F_m]) as diagnostics of leaf senescence (Oh et al., 1996). During extended dark conditions, the chlorophyll content declined more rapidly in the mutants than in the wild type and complemented mutants (Figure 2B), and it was coupled with a minor increase in the chlorophyll *a/b* ratio, a typical feature of senescence-related chlorophyll breakdown in *Arabidopsis* (Pružinská et al., 2005) (Figure 2C). Accordingly, these results were associated with a more rapid decline in the photochemical efficiency of photosystem II (PSII) (F_v/F_m) in the mutants (Figure 2D). During extended dark treatment, progression of senescence was also followed by loss of protein content
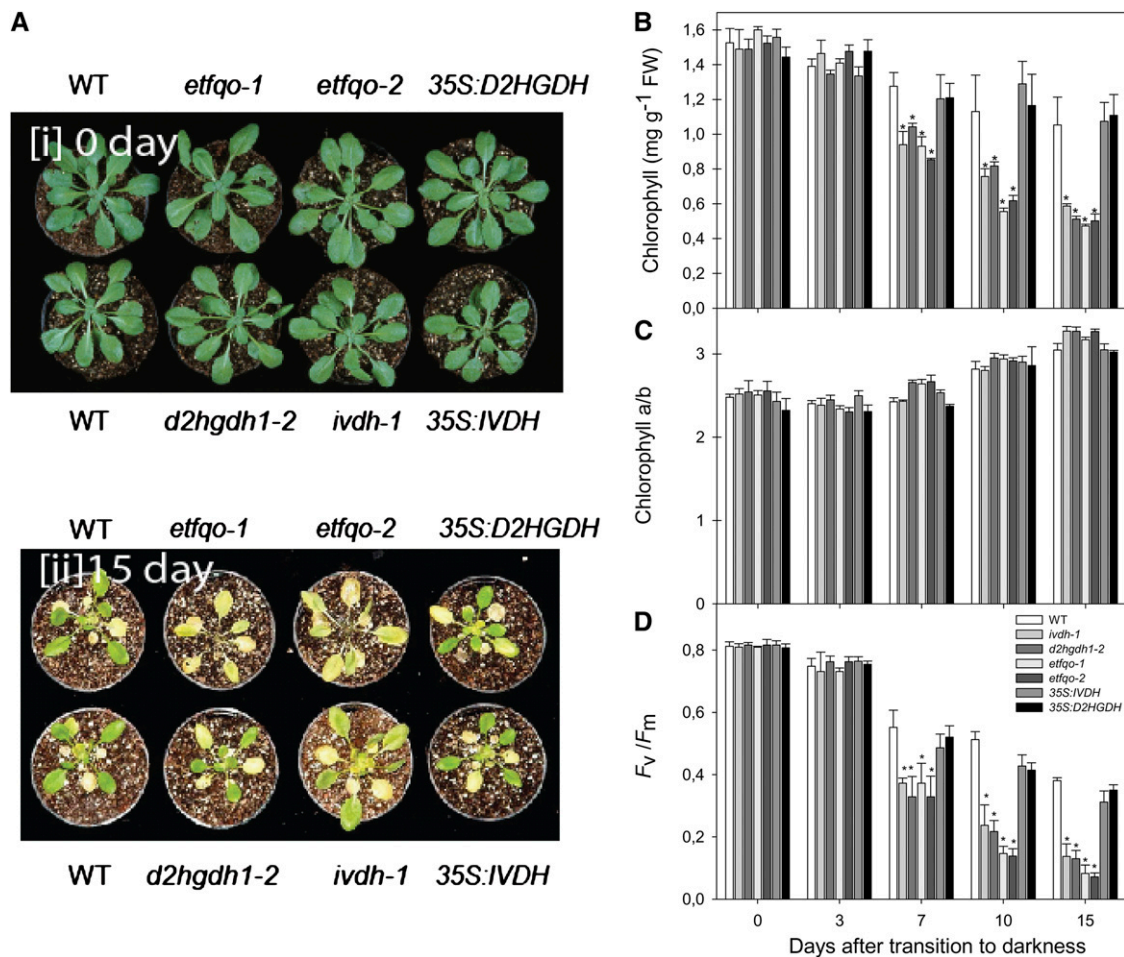

Figure 2. Phenotype of *Arabidopsis* Mutants under Extended Dark Treatment.

(A) Images of 4-week-old, short-day-grown *Arabidopsis* plants immediately (0 d) and after further treatment for 15 d in darkness conditions. The leaves of the ETFQO mutants *etfqo-1* and *etfqo-2* and of the *ivdh-1* mutant were yellowed and dehydrated following 15 d of growth in darkness compared with the wild-type (WT) control (Col-0). Additionally, the complemented lines of each genotype rescue the wild-type phenotype observed under darkness conditions.

(B) to **(D)** Chlorophyll content **(B)**, chlorophyll *a/b* ratio **(C)**, and F_v/F_m **(D)**, the maximum quantum yield of PSII electron transport, of leaves of 4-week-old, short-day-grown, *Arabidopsis* plants after further treatment for 0, 3, 7, 10, and 15 d in extended darkness. Values are means ± SE of six independent samplings; an asterisk indicates values that were determined by the Student's *t* test to be significantly different (P < 0.05) from the wild type. FW, fresh weight.

(see Supplemental Figure 1 online). It should be noted that all genotypes used in this study showed similar levels of starch, nitrate, amino acids, and proteins in samples harvested immediately prior to the start of the dark treatment (see Supplemental Table 1 online) and most importantly that complemented lines rescue the wild-type phenotype observed under darkness conditions.

Involvement of *ivdh* and *d2hgdh* in Phytol Degradation during Dark-Induced Starvation

Since one of the major functions of the ETF/ETFQO system in mammals has been shown to allow respiration of substrates other than glucose, we further analyzed changes in the fatty acid composition of leaf glycolipids during the extended dark treatment. All lines showed a typical distribution of leaf fatty acids, the predominant being the polyunsaturated fatty acids 16:3 and 18:3 (Figure 3). During the extended dark treatment, the changes in fatty acid composition of the mutants were very similar to those observed in wild-type plants.

Disruption of the electron transfer function presumably compromises dehydrogenase activity and leads to accumulation of the isovaleryl-CoA substrate. In mammals, defects in ETFQO result in a functional deficiency of mitochondrial flavoprotein dehydrogenases and accumulation of their substrates (Frerman and Goodman, 2001). To gain further insight into the functional linkage between the ETF/ETFQO system and IVDH as well as D2HGDH in *Arabidopsis*, the method of Larson and Graham (2001) was used to analyze changes in acyl-CoAs in the mutants and wild type during the extended dark treatment. The results shown in Figure 4 generally demonstrate no obvious differences between the wild type and mutants for the typical suite of medium- to long-chain acyl CoAs. However, the results presented in Figure 5 demonstrate a dramatic increase in the amounts of phytanoyl-CoA and isovaleryl-CoA in the *ivdh-1* and *etfqo* mutants, whereas in the wild type and *d2hgdh1-2* plants, these metabolites were largely unaltered. This result thus confirms the involvement of the ETF/ETFQO pathway in Leu catabolism as well as in phytol degradation during carbohydrate deprivation; however, it rules out the possibility that D2HGDH plays a major role, if any, in these catabolic pathways. Of further note is the marked accumulation of 2-hydroxyglutarate in the *d2hgdh1-2* and *etfqo* mutants, suggesting a linkage between 2-hydroxyglutarate metabolism and the ETF/ETFQO system.

Metabolic Profile of *ivdh-1* and *d2hgdh1-2* Lines during Dark-Induced Starvation

Further metabolic characterization of the accelerated senescence phenotype in the mutants was performed using an established gas chromatography–mass spectrometry (GC-MS) metabolic profiling protocol (Lisec et al., 2006). The extended dark treatment led to a rapid decline in sucrose and other sugars in all genotypes analyzed (Figure 6). The TCA cycle intermediates citrate, isocitrate, malate, fumarate, and succinate generally increased at the end of dark treatment (Figure 6). By contrast, the levels of 2-oxoglutarate and dehydroascorbate were dramatically reduced, declining to as low as 10% of the level measured

at the start of the dark treatment. While these changes are striking, the exact mechanism underlying this phenomenon cannot be elucidated from the results in this study. However, there are two possible explanations to account for the changes in the amounts of these metabolites. First, it is conceivable that the TCA cycle is progressively upregulated in the mutant, during the course of the extended darkness, in an attempt to compensate for the reduced availability of respiratory substrate. Second, the accumulation of TCA cycle intermediates may be a consequence of a general downregulation of biosynthesis that would be anticipated under conditions of carbon starvation.

It is of interest that most of the free amino acids increased significantly in all genotypes during the darkness, including Arg, Asn, Ala, γ-amino butyric acid (GABA), Leu, Ile, Lys, Phe, Ser, Thr, Tyr, Trp, and Val, indicating an increased protein degradation (and subsequent metabolism in the case of GABA) under the experimental conditions (Figure 7). The significantly elevated levels of several amino acids, especially the branched-chain amino acids, aromatic amino acids, and Lys, in the mutants indicate the involvement of the ETF/ETFQO pathway in their degradation. However, the levels of Glu, 2-oxoglutarate, and pyroglutamate declined in all mutants at 7 to 10 d, whereas they increased in the wild type (Figures 6 and 7). When taken together with the elevated levels of GABA, these data are likely indicative of an upregulation of the GABA shunt as an alternative source of mitochondrial succinate (Studart-Guimarães et al., 2007).

Involvement of *ivdh1-2* and *d2hgdh1-2* in Leu Catabolism

To elucidate further the connection between ETF/ETFQO and IVDH/D2HGDH-mediated metabolism, we performed isotope labeling experiments in which we evaluated the relative isotope redistribution in leaves excised from wild-type and mutant plants at various time points throughout dark treatment. For this purpose, we used a combination of feeding [U-13C]-labeled substrate ([U-13C]-Val and [U-13C]-Lys) to the leaf via the transpiration stream and a recently adapted GC-MS protocol that facilitates isotope tracing (Roessner-Tunali et al., 2004). Interestingly, the changes in redistribution of isotope were essentially conserved across the mutants, with results from this experiment in close agreement with the observed alteration in the steady state levels of sugars, organic acids, and amino acids (Figures 6 and 7). That said, certain differences were observed between the mutants and the wild type (Figure 8). Following feeding of ([U-13C]-Val, it is clear that the branched-chain amino acid–derived branched-chain keto acids increase only in the *ivdh-1* and *etfqo* mutants. The same is true for [U-13C]-Lys feeding in the case of α-ketovalerate but not α-ketoisocaproate. Following feeding of either Val or Lys, considerable label accumulated as 2-hydroxyglutarate in *d2hgdh1-2* and *etfqo* mutants, but a much greater total accumulation was observed in the latter (Figure 8).

DISCUSSION

We and others have previously suggested that IVDH and D2HGDH provide electrons to the plant ubiquinol pool via the ETF/ETFQO complex on the basis of the accumulation of
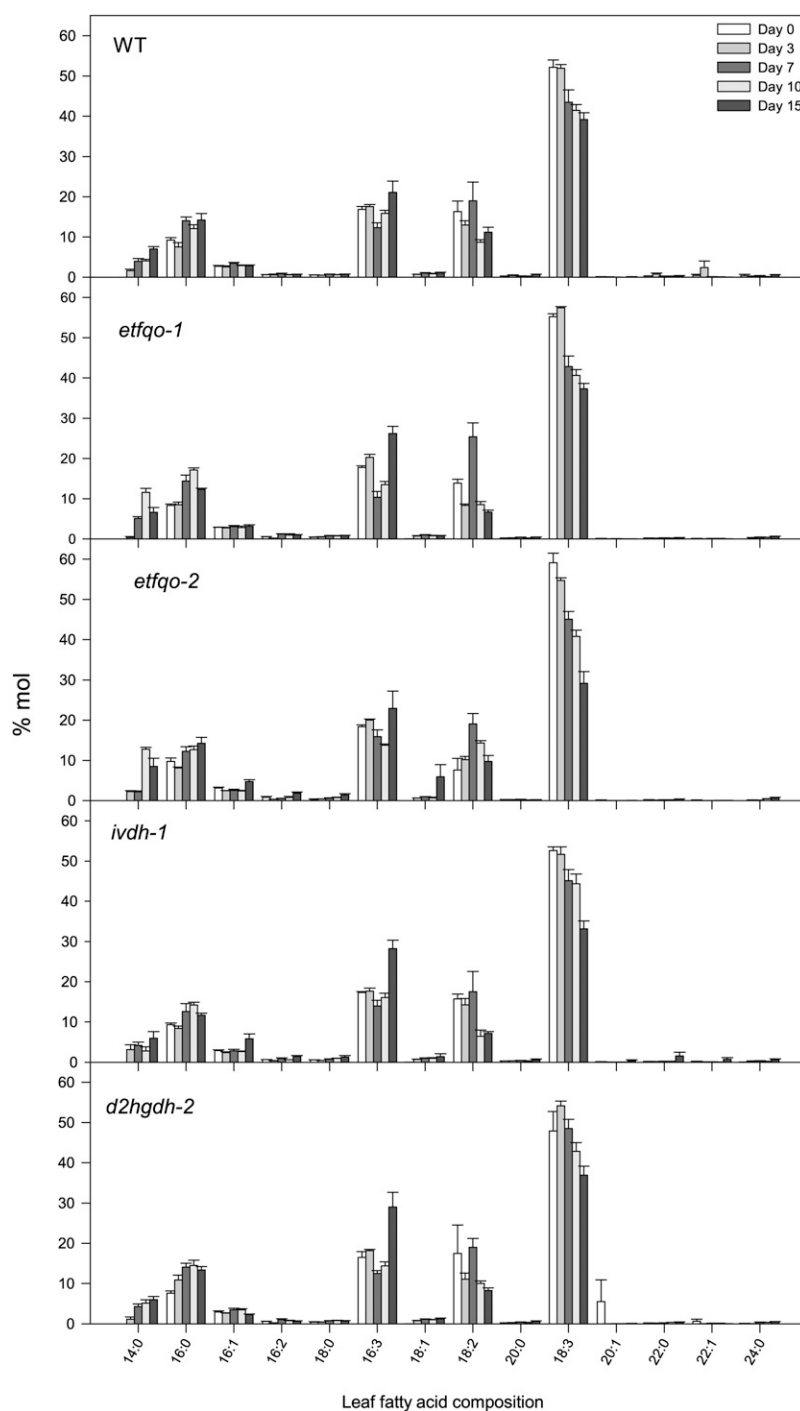
Figure 3. Leaf Fatty Acid Composition in *Arabidopsis* Mutants under Extended Dark Treatment.

Data (in mol %) represent mean ± SE for six independent samplings of 9th or 10th leaves of 4-week-old, short-day-grown *Arabidopsis* plants after treatment for 0, 3, 7, 10, and 15 d in extended darkness. Fatty acid composition was analyzed by GC of fatty acid methyl esters. WT, wild type.
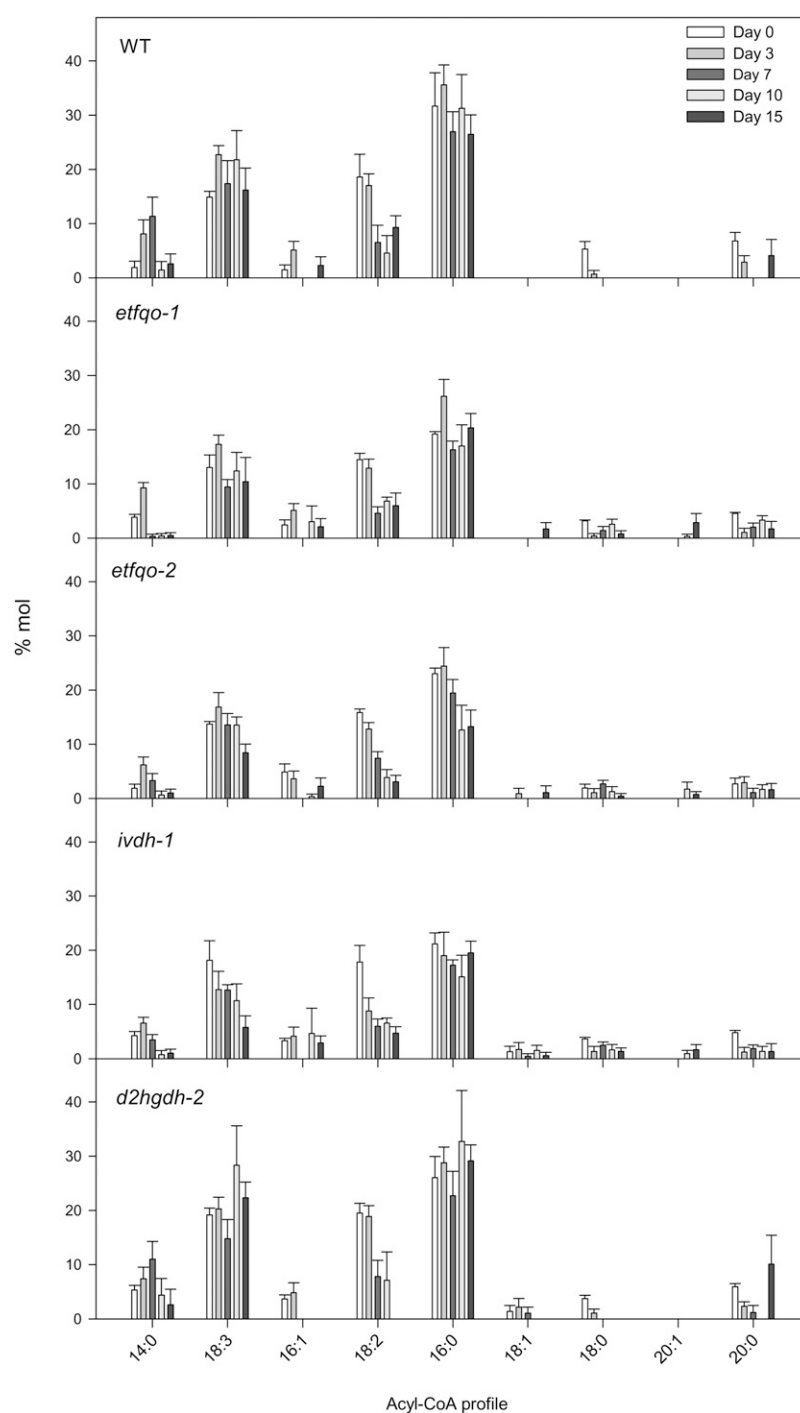
Figure 4. Acyl-CoA Profiles in *Arabidopsis* Mutants under Extended Dark Treatment.

Data (in mol %) represent means ± SE for six independent samplings of the 9th or 10th leaves of 4-week-old, short-day-grown *Arabidopsis* plants after further growth for 0, 3, 7, 10, and 15 d in extended darkness. Samples of 10 mg (fresh weight) each were derivatized to their acyl-etheno-CoA esters, separated by HPLC, and detected fluorometrically. WT, wild type.
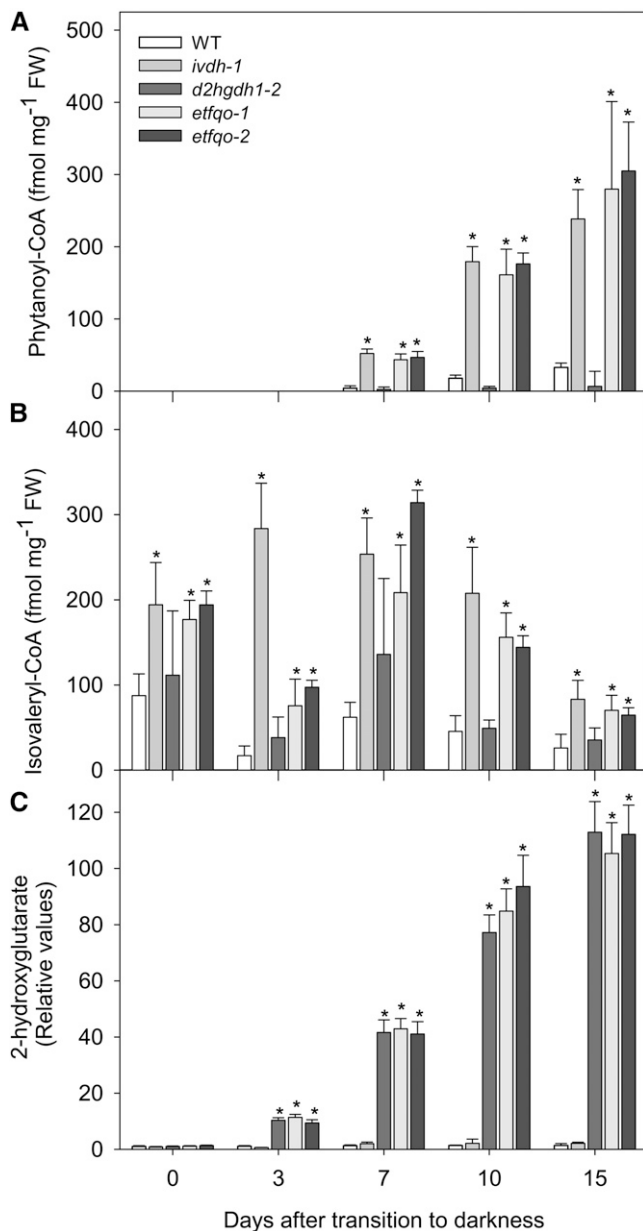
Figure 5. Metabolic Phenotype of *Arabidopsis* Mutants in Extended Dark Treatment.

Phytanoyl-CoA **(A)**, isovaleryl-CoA **(B)**, and 2-hydroxyglutarate **(C)** profiles in *Arabidopsis* mutants under extended dark treatment. Samples were taken from leaves of 4-week-old, short-day-grown *Arabidopsis* plants after treatment for 0, 3, 7, 10, and 15 d in extended darkness. Values are means ± SE of six independent samplings; an asterisk indicates values that were determined by the Student's *t* test to be significantly different (P < 0.05) from the wild type (WT). FW, fresh weight.

isovaleryl-CoA and coexpression analysis of microarray data sets, respectively (Ishizaki et al., 2005; Engqvist et al., 2009). Moreover, D2HGDH has been shown to be a part of the suite of enzymes acting as electron donors to this complex in humans (Struys et al., 2005). More recently, key roles for this enzyme in

certain types of human cancer (Dang et al., 2009) and in neurological disorders (O'Connor et al., 2009) have been proposed. Using fluorescent labeling and proteomics analysis, both enzymes have been shown to reside in the mitochondria (Däschner et al., 2001; Heazlewood et al., 2004). Here, we provide experimental evidence to support the participation of both enzymes during the induction of alternative respiration following prolonged carbon starvation by characterizing their respective *Arabidopsis* knockout mutants.

One piece of evidence for the participation of the two enzymes in the alternative respiration pathway is that they display a similar, yet milder, early onset of dark-induced senescence as evidenced both by the visual phenotype of plants following growth in extended periods of darkness and by the loss of chlorophyll and photosynthetic competence (Figure 2). Interestingly, *ivdh-1* plants exhibit a stronger phenotype than do the *d2hgdh1-2* plants. Since both enzymes are encoded by single genes, this finding suggests that IVDH likely exerts a greater share of the control of electron provision to the ETF/ETFQO complex than does D2HGDH. That said, the fact that the effects were relatively strong in both mutants suggests that they are the most important electron donors to this complex in plants. Our data also allowed us to dissect upstream events linking the well-characterized mobilization of chlorophyll, fatty acids, and protein during dark-induced senescence (Ishizaki et al., 2005; Kunz et al., 2009; Schelbert et al., 2009). In our previous metabolic studies on knockout mutants of the ETF and ETFQO proteins, we reported that in the absence of a functional ETF/ETFQO complex, there was a marked accumulation of branched-chain amino acids, aromatic amino acids, phytanoyl-CoA, and isovaleryl-CoA (Ishizaki et al., 2005, 2006). The enzymology of plant D2HGDH, catalyzing the conversion of D-2-hydroxyglutarate to 2-oxoglutarate, has recently been described and in conjunction with an analysis of coexpression of genes in microarrays, has been postulated to play a role in phytol, odd-chain fatty acid, and branched-chain amino acid degradation (Engqvist et al., 2009). Our measurements of the levels of the substrate of this enzyme, 2-hydroxyglutarate, revealed that it also massively accumulated in the *etfqo* and *d2hgdh1-2* mutants but not in the *ivdh-1* mutant; moreover, phytanoyl-CoA accumulates in all the mutants except *d2hgdh1-2* (Figure 5). These data thus demonstrate that D2HGDH is not involved in the catabolism of these metabolites but that this is exclusively mediated by IVDH, implying that the enzymes operate in two separate albeit functionally similar pathways. The isotope tracer experiments we performed further confirm that branched-chain amino acid catabolism proceeds through IVDH (Figure 8).

Another observation here that we did not comment on in our previous studies was the apparent upregulation of the GABA shunt. While the role of GABA in plants is not yet fully understood, it is clearly an important pathway under times of stress (Bouche and Fromm, 2004; Fait et al., 2008), and recent studies have shown that the GABA shunt is responsible for a considerable proportion of mitochondrial succinate production (Studart-Guimarães et al., 2007). Under normal growth conditions, Glu is converted via the plastidial Asp family pathway into Met, Thr, Ile, and Lys (Fait et al., 2008). Stress conditions induce the expression of the bifunctional polypeptide Lys-ketoglutarate reductase
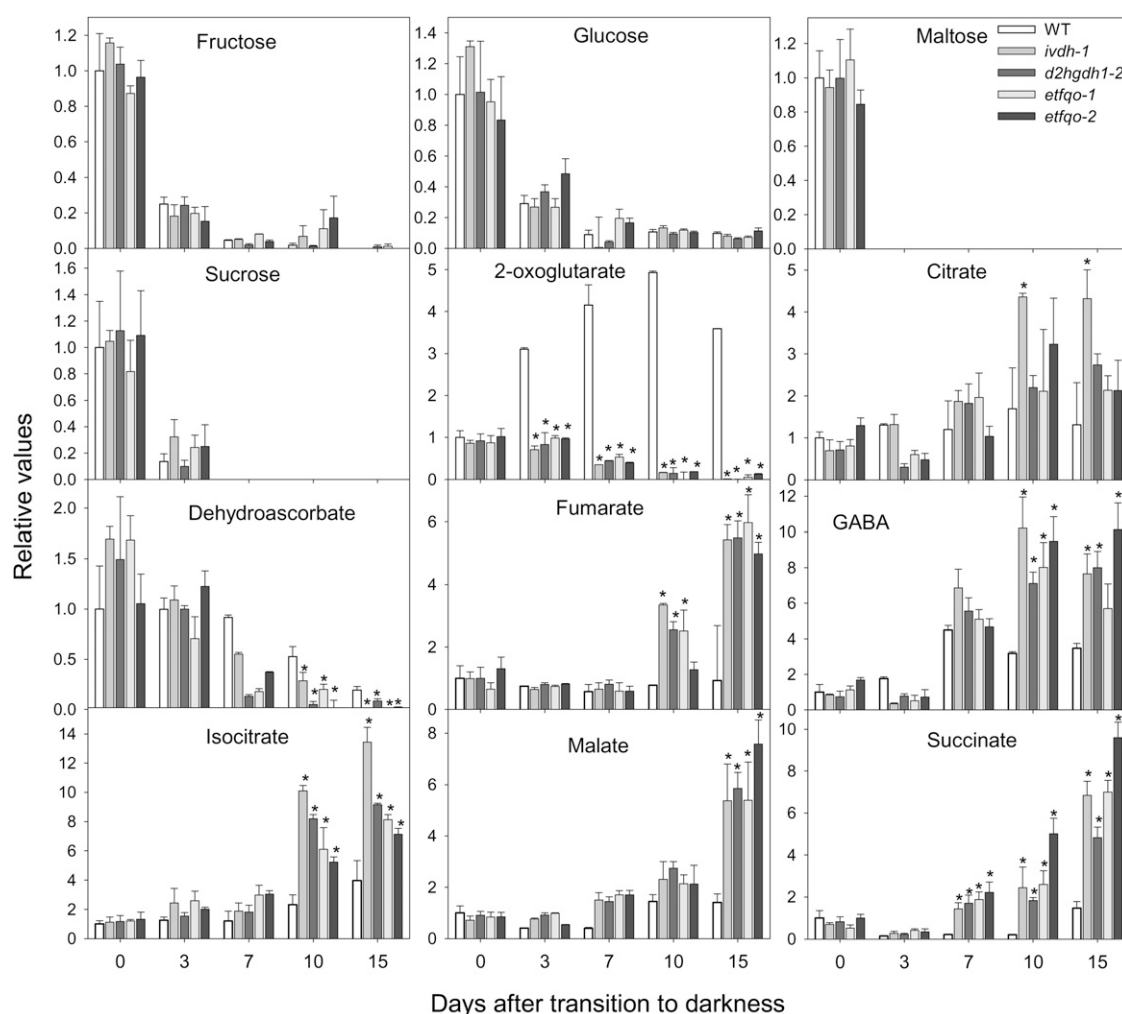
Figure 6. Relative Levels of Sugars and Organic Acids in *Arabidopsis* Mutants during Extended Dark Conditions as Measured by GC-MS.

The *y* axis values represent the metabolite level relative to the wild type (WT). Data were normalized to the mean response calculated for the 0-d dark-treated leaves of the wild type. Values presented are means ± SE of determinations on six independent samplings; an asterisk indicates values that were determined by the Student's *t* test to be significantly different (P < 0.05) from the wild type.

and saccharopine dehydrogenase (LKR/SDH) involved in the catabolism of Lys (Stepansky et al., 2006). Moreover, bioinformatic analyses have revealed that the TCA cycle and GABA shunt are differentially regulated at the level of gene expression (Fait et al., 2008). It thus seems reasonable to assume that the increased GABA levels are occurring in response to changing environmental conditions (Fait et al., 2008) and represent another adaptive mechanism for maintaining the rate of respiration in these genotypes.

A detailed understanding of the mechanisms of chlorophyll and phytol degradation is still lacking (Hörtensteiner, 2006); nevertheless, our results clearly indicate a role for IVDH in this process. Because of the lack of major changes in their steady state levels, however, we were unable to assign unambiguously anaplerotic fatty acid breakdown to either metabolic route (Figure 3). By contrast, it appears that both IVDH and D2HGDH play roles in the degradation of the aromatic amino acids (Figure 7)

since they accumulate to relatively high levels in both mutants. Given the strong interconnections of the network of plant amino acid metabolism (Zhu and Galili, 2003; Gu et al., 2010), this observation is perhaps unsurprising. It does, however, mean that considerable work is still required to achieve mechanistic understanding of this phenomenon.

While the process of Lys degradation is not, as yet, fully understood, a range of important studies in plants and mammals precede our work (Galili et al., 2001; Mills et al., 2006; Stepansky et al., 2006; Zinnanti et al., 2007; Angelovici et al., 2009; Struys and Jakobs, 2010). Current knowledge of mammalian Lys catabolism is largely based on a range of studies in different species in which [14C]-labeled Lys was supplied as tracer (Ghadimi et al., 1971; Chang, 1982). These studies, alongside a more recent 15N study (Struys and Jakobs, 2010), have facilitated the elucidation of the entire degradative pathway in mammals. In plants, the presence of a Lys catabolism pathway was confirmed
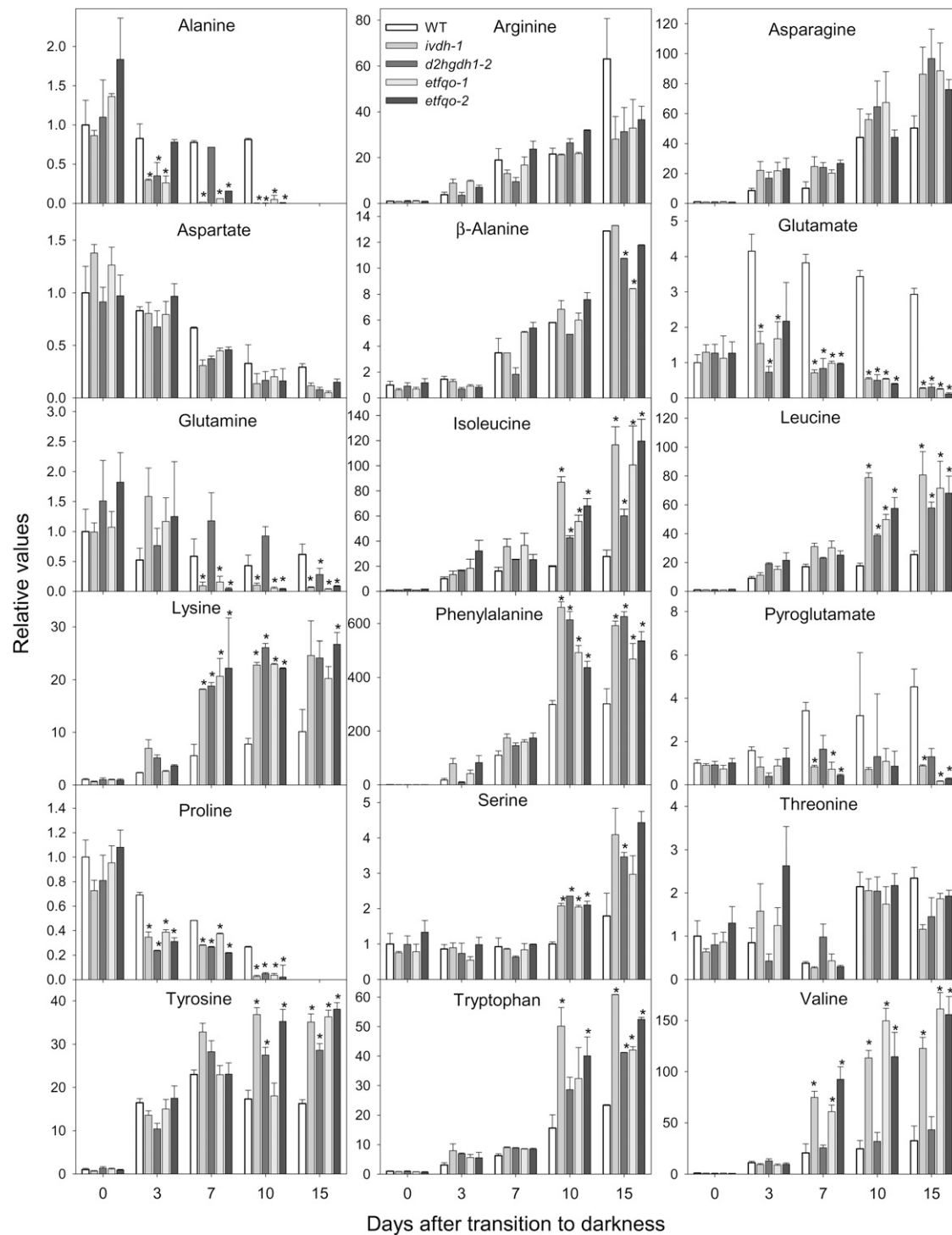
Figure 7. Relative Levels of Amino Acids in *Arabidopsis* Mutants during Extended Dark Conditions as Measured by GC-MS.

Levels of the indicated amino acids are presented as in Figure 6. WT, wild type.
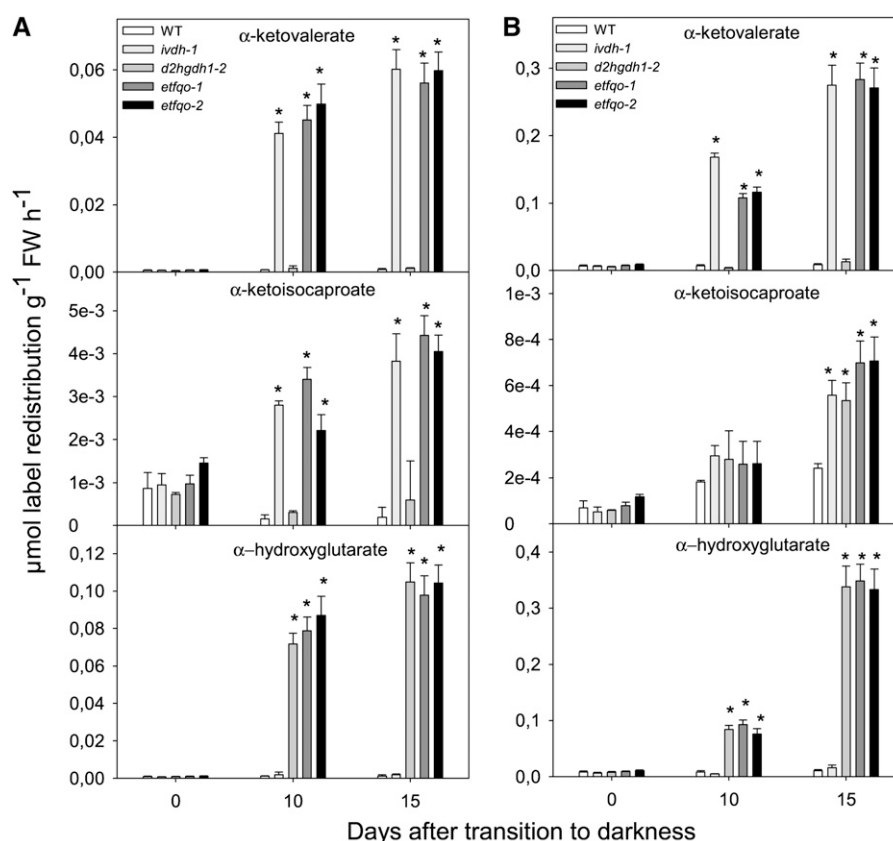
Figure 8. Redistribution of Heavy Label Following Amino Acid Feeding of *Arabidopsis* Mutant and Wild-Type Leaves.

The 9th or 10th leaves of 4-week-old, short-day-grown *Arabidopsis* plants after treatment for 0, 10, or 15 d in extended darkness were harvested and fed via the petiole with either [U-^{13}C]-Val **(A)** or [U-^{13}C]-Lys **(B)** solution. Values represent absolute redistribution of the label and are given as means $\pm$ SE of determinations on six independent samplings; an asterisk indicates values that were determined by the Student's *t* test to be significantly different (P < 0.05) from the wild type. FW, fresh weight.

using the same approach, which revealed that [^{14}C] label fed to barley (*Hordeum vulgare*) seeds was converted into Glu and α-amino adipic semialdehyde (Sodek and Wilson, 1970; Brandt, 1975). In addition, numerous approaches have been taken to boost the Lys content in plants (Azevedo and Lea, 2001; Galili et al., 2001; Ufaz and Galili, 2008), and for this reason, the degradative pathway has also been targeted. In one such strategy, a series of transgenic maize (*Zea mays*) plants overaccumulating Lys were produced using distinct strategies, including an endosperm-specific RNA interference suppression of LKR/ SDH (Houmard et al., 2007; Frizzi et al., 2008; Reyes et al., 2009). Most approaches that led to accumulation of Lys also led to a concomitant degradation of Lys, resulting in the formation of saccharopine and α-aminoadipate δ-semialdehyde (Falco et al., 1995; Houmard et al., 2007; Frizzi et al., 2008; Azevedo and Arruda, 2010). When taken together with our work here, these studies demonstrate the functionality of the currently accepted pathway of Lys degradation in plants (see Supplemental Figure 2 online). In addition, our data allow us to postulate a second independent pathway of degradation that is responsible for carrying a considerable proportion of the Lys degradative flux (discussed in detail below).

Lys also accumulated in both the *ivdh-1* and *d2hgdh1-2* mutants during extended darkness, suggesting that its catabolic products can follow either route to the ETF/ETFQO complex. The Lys degradative pathway in plants is relatively poorly characterized with the exception of the exquisite multilayered regulation exerted by the initial reaction catalyzed by the bifunctional Lys ketoglutarate reductase/saccharopine dehydrogenase, which degrades Lys to form Glu and α-aminoadipate δ-semialdehyde (Galili et al., 2001). Our observations suggest that Lys degradation occurs via a branched pathway partially similar to that described for the bacteria *Rhodospirillum rubrum* (Ebisuno et al., 1975) and recently described in mammalian systems (Struys and Jakobs, 2010) with 2-hydroxyglutarate being produced via a pipecolate pathway and branched-chain keto acids being produced via an as yet undefined aminotransferase (see Supplemental Figure 2 online). The results of our Lys feeding experiment (Figure 8) suggest that α-ketovalarate is a good candidate product for such an aminotransferase and essentially allows us to exclude α-ketoisocaproate. Intriguingly, they also suggest that the proportion of Lys degraded via the α-ketovalarate route is quantitatively equivalent to that degraded via the 2-hydroxyglutarate route. Interestingly, in
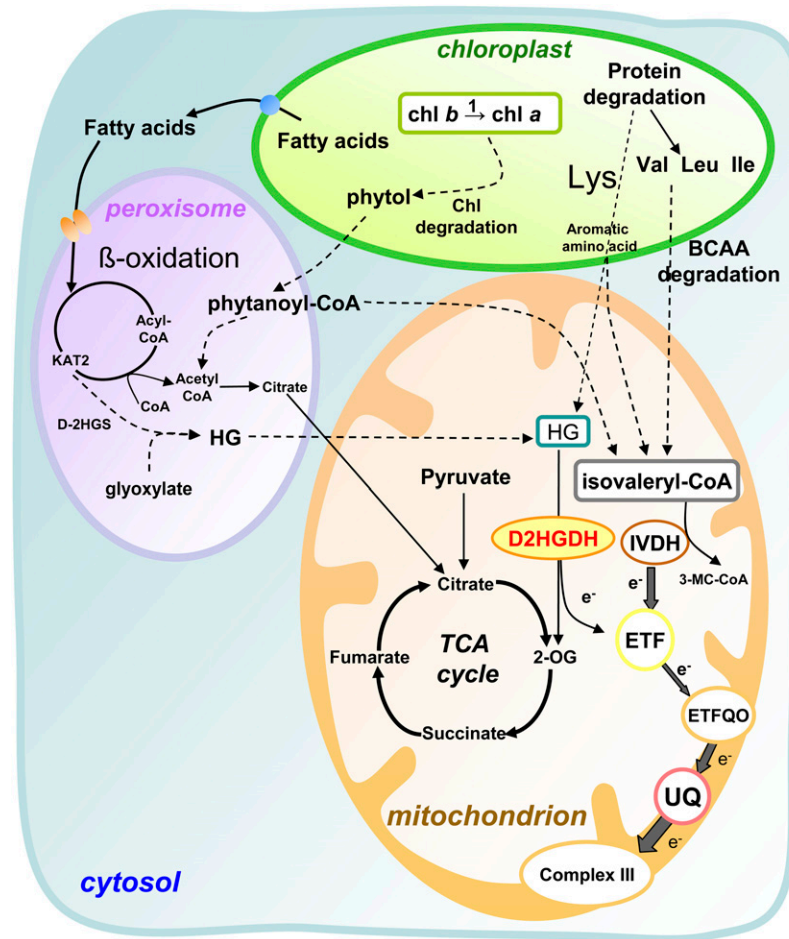
Figure 9. Metabolic Model Showing the Involvement of IVDH and D2HGDH in Feeding Electrons to the Mitochondrial Respiration Electron Chain.

Isovaleryl-CoA may be produced by BCAA catabolism, chlorophyll degradation, and/or Lys degradation, whereas HG can be produced either in the peroxisome or from the Lys derivative L-pipecolate as in nonplant systems. Thus, the electrons generated are transferred to the respiratory chain through the ubiquinol pool via an ETF/ETFQO system. Dotted arrows represent possible transport processes. *2-OG*, 2-oxoglutarate; HG, D-2-hydroxyglutarate; *e-*, electron; *UQ*, ubiquinone; 3-MC-CoA, 3-methylcrotonyl-CoA; KAT2, keto-acyl-thiolase 2; chl, chlorophyll; D-2HGS, 2-hydroxyglutarate synthase; 1, conversion of chlorophyll *b* to *a* by chlorophyll *b* reductase.

mammals an α-aminoadipate δ-semialdehyde dehydrogenase, also named antiquitin, has been described in the pipecolic acid pathway of Lys catabolism (Mills et al., 2006). Deficiency of antiquitin causes seizures because accumulating Δ^1-piperideine-6-carboxylate condenses with pyridoxal 5′-phosphate and inactivates this enzyme cofactor, which is essential for normal metabolism of neurotransmitters (Mills et al., 2006; Struys and Jakobs, 2010). However, future genetic studies are still required to assess the importance of this enzyme in plants.

In an attempt to identify further candidate genes involved in adaptation to dark-induced senescence, we performed a coexpression analysis using genes known to be involved in β-oxidation branched-chain amino acid degradation, *IVDH*, *D2HGDH*, and the Lys catabolism gene *LKR/SDH* (see Supplemental Figure 3 and Supplemental Table 2 online). As would perhaps be expected, from the previous work of Engqvist et al. (2009), this analysis revealed tight connections between Lys

catabolism and the other pathways, particularly in the case of clusterings performed on data from developmental or stress experiments. Nineteen genes that show a similar pattern of expression to *LKR/SDH* and *D2HGDH* were identified (see Supplemental Table 3 online); some of these represent logical candidates for an involvement in Lys degradation. However, it is important to note that caution must be taken when performing coresponse analysis (Usadel et al., 2009; Tohge and Fernie, 2010), and experimental validation of the involvement of the enzymes encoded by these genes products is still required.

As previously described (Ishizaki et al., 2005, 2006), dark-induced senescence induces the ETF/ETFQO alternative pathway of respiration. The results presented here demonstrate the enzymes IVDH and D2HGDH integrate electron donation to this complex. They do so using branched-chain and aromatic amino acids, phytol, and Lys in the case of IVDH and aromatic amino acids and Lys in the case of D2HGDH (Figure 9). We propose that

the higher substrate range of IVDH may be responsible for its more critical role in the process of dark-induced senescence. Given the importance of these pathways, we speculated that, although the ETF/ETFQO pathway is apparently not essential under our standard growth conditions (long days), it may become more relevant under specific environmental conditions or stresses. We therefore tested a variety of different growth conditions, including continuous light (24 h light/0 h dark), short-day (8 h light/16 h dark), and cold conditions (13°C, 16 h light/8 h dark) (see Supplemental Figure 4 online). In all conditions tested, the mutant plants exhibited symptoms of early senescence in comparison to the wild type. This suggests a role for the ETF/ETFQO pathway not only during the severe stress imposed by extended darkness but also under conditions experienced by most plants at some stage during their life cycle. However, it is important to note that microarray experiments comparing developmental senescence with artificially induced senescence have indicated many common features but also some significant differences (Buchanan-Wollaston et al., 2005). For instance, the signaling pathway involving the hormone salicylic acid is important in developmental senescence (Lim et al., 2007) but not in artificially induced senescence (Buchanan-Wollaston et al., 2005). In the light of this, further studies are required (1) to confirm the identity of the entire pathway of Lys degradation induced under carbon starvation, (2) to characterize the role of alternative respiration under a range of environmental stresses, and (3) to fully define the routes of aromatic amino acid and phytol breakdown during this process.

METHODS

Plant Material

All *Arabidopsis thaliana* plants used in this study were of the Col ecotype (Col-0). *Arabidopsis* seeds were handled exactly as described previously (Ishizaki et al., 2005, 2006). The T-DNA mutant lines GK756G02 (*ivdh-1*) and SAIL844G06 (*d2 hgdh1-2*, as described in Engqvist et al., 2009) were obtained from the Nottingham Arabidopsis Stock Centre (University of Nottingham, UK). The mutant lines, SALK T-DNA line SALK_007870 (*etfqo-1*), and Syngenta *Arabidopsis* insertion line SAIL_91_E03 (*etfqo-2*) were previously described (Ishizaki et al., 2005).

Isolation of T-DNA Insertion Mutants and Genotype Characterization

Homozygous mutant lines were isolated by PCR using primers specific for IVDH open reading frame (ORF) (IVDH_L, 5′-CGGGTTCAGTTGCTTT-GTCT-3′, and IVDH_R, 5′-CCAGTGTTTCAGCAGATGGA-3′) in combination with the T-DNA left border primer (GABI-LB8409, 5′-ATATTGACCA-TCATACTCATTGC-3′) for *ivdh-1*, or primers specific for *D2HGDH* (D2HGDH_L, 5′-GAAGCTGTCATATCGGTGGA-3′ and D2HGDH_R, 5′-TCGTACCCAGTATTGTCTTTGC-3′) in combination with the T-DNA left border primer (TMR1_LB1, 5′-GCCTTTTCAGAAATGGATAAATAG-CCTTGCTTCC-3′) for *d2hgdh1-2*.

Complementation of the Mutant Lines with Cauliflower Mosaic Virus 35S Promoter-Driven ORFs

The full-length ORFs including stop codons of *IVDH* and *D2HGDH* were amplified by PCR from the wild type and subcloned into the pH2GW7 vector (www.psb.ugent.be/gateway) (Karimi et al., 2002) using the GATE-WAY recombination system (Invitrogen). Homozygous plants both of the *ivdh-1* and *d2hgdh1-2* mutants were transformed with their respective complementing vector by *Agrobacterium tumefaciens*–mediated gene transfer using the floral dip method (Clough and Bent, 1998). Homozygous *ivdh-1* lines containing the cauliflower mosaic virus 35S promoter-driven *IVDH* ORF were characterized by genomic PCR using the primer set IVDH_L and IVDH_R described above to check the transformed *IVDH* ORF and the primer set IVDH_L and IVDH_RI (5′-TCTCAAACTCTT-GATCCGAAAA-3′) to confirm that there was no amplification from a disrupted copy of *IVDH*. Homozygous *d2hgdh1-2* lines containing the cauliflower mosaic virus 35S promoter-driven *D2HGDH* ORF were characterized by genomic PCR using the primer set D2HGDH_L and D2HGDH_R described above to check the transformed *D2HGDH* ORF and the primer set D2HGDH_L and D2HGDH_RI (5′-CAAGCACAAGC-CAATATAATACC-3′) to confirm that there was no amplification from a disrupted copy of *D2HGDH*.

Analysis of *ETFQO* mRNA Expression by RT-PCR

Total RNA was isolated from rosette leaves of 3 d dark-treated plants using TRIzol reagent. First-strand cDNA was synthesized from 10 μg of total RNA with Superscript II Rnase H⁻ reverse transcriptase (Invitrogen) and oligo (dT) primer. PCR amplification of cDNA-specific sequence was performed using primers specific for the ORF, L and R, described above. PCR amplification of the cDNA encoding the β-tubulin of *Arabidopsis* (*TUB9*) with a forward primer (5′-GATATCTGTTTCCGTACCTTGAAGC-3′) and a reverse primer (5′-CCGACTGTAGCATCTTGATATTGC-3′) served as a control.

Dark Treatment

For dark treatments, 7- to 10-d-old seedlings were transferred to soil and then grown at 22°C under short-day conditions (8 h light/16 h dark) for 4 weeks. Following bolting, plants were grown at 22°C in the dark in the same growth cabinet. The fully expanded 9th to 12th rosette leaves were harvested at intervals of 0, 3, 7, 10, and 15 d from control and dark-grown plants for subsequent analysis. Additionally, the experiment was repeated at least four times (six in the case of the *etfqo* mutants, even in different growth facilities) with similar phenotypes observed each time.

Measurement of Senescence Parameters

Chlorophyll content was determined as described in the literature (Porra et al., 1989) and the protein content as in Bradford (1976). The ratio of F_v to F_m, which corresponds to the potential quantum yield of the photochemical reactions of PSII, was measured as previously described (Oh et al., 1996) as a measure of the photochemical efficiency. Starch, nitrate, and total amino acids were determined as by Sienkiewicz-Porzucek et al. (2010).

Acetyl-CoA and Fatty Acid and Polar Primary Metabolite Profiling

Acyl-CoAs, fatty acids, and polar primary metabolites were extracted and evaluated exactly as previously described (Ishizaki et al., 2005), with the exception that additional peaks were looked for in the GC-MS chromatograms of the polar primary metabolites using the libraries housed in the Golm Metabolome Database (Kopka et al., 2005; Schauer et al., 2005).

Extraction, Derivatization, and Analysis of *Arabidopsis* Leaf Metabolites Using GC-MS

Metabolite extraction for GC-MS was performed by a method modified from that described by Roessner-Tunali et al. (2003). *Arabidopsis* leaf

tissue (~180 mg) was homogenized using a ball mill precooled with liquid nitrogen and extracted in 1400 μL of methanol, and 60 μL of internal standard (0.2 mg ribitol mL^{-1} water) was subsequently added as a quantification standard. The extraction, derivatization, standard addition, and sample injection were exactly as described previously (Lisec et al., 2006). Both chromatograms and mass spectra were evaluated using either TAGFINDER (Luedemann et al., 2008) or the MASSLAB program (ThermoQuest), and the resulting data were prepared and presented as described by Roessner et al. (2001).

Analysis of [U-^{13}C]-Val and [U-^{13}C]-Lys Labeled Samples

Arabidopsis leaves of similar size (the fully expanded 9th to 10th rosette leaves) but from different genotypes and following varying lengths of darkness treatment were fed via the petiole with 20 mM [U-^{13}C]-Lys or 20 mM [U-^{13}C]-Val (both from Cambridge Isotope Laboratories) by incubation in buffered solution (10 mM MES-KOH, pH 6.5) for a period of 6 h. At the end of the incubation, leaves were snap-frozen in liquid nitrogen. They were subsequently extracted in 100% methanol and processed exactly as described by Timm et al. (2008). The metabolic fate of these substrates was subsequently assessed exactly as described previously (Tieman et al., 2006).

Accession Numbers

The Arabidopsis Genome Initiative locus numbers for the major genes discussed in this article are as follows: IVDH, At3g45300; D2HGDH, At4g364000; and ETFQO, At2g43400. Others genes discussed in this article are shown in Supplemental Table 2 online.

Supplemental Data

The following materials are available in the online version of this article.

   Supplemental Figure 1. Protein Content in *Arabidopsis* Mutants under Extended Dark Treatment.

   Supplemental Figure 2. Metabolic Pathway of Lys Degradation in Plants Showing the Involvement of D2HGDH in Feeding Electrons to the Mitochondrial Electron Transport Chain.

   Supplemental Figure 3. A Coexpression Analysis Using Genes for β-Oxidation, Branched-Chain Amino Acid Degradation, Chlorophyll Breakdown, and the Lys Catabolism Gene.

   Supplemental Figure 4. Natural Senescence Phenotype of *Arabidopsis* Mutants under Different Growth Conditions.

   Supplemental Table 1. Metabolite Levels in *Arabidopsis* Mutants.

   Supplemental Table 2. Accession Numbers of *Arabidopsis* Genes Used in This Article for Coexpression Analysis.

   Supplemental Table 3. List of Candidate Genes for Involvement in Lys Degradation.

REFERENCES

Achouri, Y., Noel, G., Vertommen, D., Rider, M.H., Veiga-Da-Cunha, M., and van Schaftingen, E. (2004). Identification of a dehydrogenase acting on D-2-hydroxyglutarate. Biochem. J. **381:** 35–42.

Angelovici, R., Fait, A., Zhu, X., Szymanski, J., Feldmesser, E., Fernie, A.R., and Galili, G. (2009). Deciphering transcriptional and metabolic networks associated with lysine metabolism during Arabidopsis seed development. Plant Physiol. **151:** 2058–2072.

Azevedo, R.A., and Arruda, P. (April 7, 2010). High-lysine maize: the key discoveries that have made it possible. Amino Acids, http://dx.doi.org/10.1007/s00726-010-0576-5.

Azevedo, R.A., and Lea, P.J. (2001). Lysine metabolism in higher plants. Amino Acids **20:** 261–279.

Beckmann, J.D., and Frerman, F.E. (1985). Electron-transfer flavoprotein:ubiquinone oxidoreductase from pig liver: Purification and molecular, redox, and catalytic properties. Biochemistry **24:** 3913–3921.

Bouche, N., and Fromm, H. (2004). GABA in plants: Just a metabolite? Trends Plant Sci. **9:** 110–115.

Bradford, M.M. (1976). A rapid and sensitive method for quantitation of microgram quantities of protein utilizing the principle of protein-dye-binding. Anal. Biochem. **72:** 248–254.

Brandt, A.B. (1975). *In vivo* incorporation of lysine-C^{14} into the endosperm of wild type and high lysine barley. FEBS Lett. **52:** 288–291.

Buchanan-Wollaston, V., Page, T., Harrison, E., Breeze, E., Lim, P.O., Nam, H.G., Lin, J.-F., Wu, S.-H., Swidzinski, J., Ishizaki, K., and Leaver, C.J. (2005). Comparative transcriptome analysis reveals significant differences in gene expression and signalling pathways between developmental and dark/starvation-induced senescence in Arabidopsis. Plant J. **42:** 567–585.

Chang, Y.F. (1982). Lysine metabolism in the human and the monkey: Demonstration of pipecolic acid formation in the brain and other organs. Neurochem. Res. **7:** 577–588.

Clough, S.J., and Bent, A.F. (1998). Floral dip: A simplified method for Agrobacterium-mediated transformation of *Arabidopsis thaliana.* Plant J. **16:** 735–743.

Dang, L., et al. (2009). Cancer-associated IDH1 mutations produce 2-hydroxyglutarate. Nature **462:** 739–744.

Däschner, K., Couée, I., and Binder, S. (2001). The mitochondrial isovaleryl-coenzyme A dehydrogenase of Arabidopsis oxidizes intermediates of leucine and valine catabolism. Plant Physiol. **126:** 601–612.

Ebisuno, T., Shigesada, K., and Katsuki, H. (1975). D-α-hydroxyglutarate dehydrogenase of *Rhodospirillum rubrum.* J. Biochem. **78:** 1321–1329.

Engqvist, M., Drincovich, M.F., Flügge, U.I., and Maurino, V.G. (2009). Two D-2-hydroxy-acid dehydrogenases in *Arabidopsis thaliana* with catalytic capacities to participate in the last reactions of the methylglyoxal and beta-oxidation pathways. J. Biol. Chem. **284:** 25026–25037.

Fait, A., Fromm, H., Walter, D., Galili, G., and Fernie, A.R. (2008). Highway or byway: The metabolic role of the GABA shunt in plants. Trends Plant Sci. **13:** 14–19.

Falco, S.C., Guida, T., Locke, M., Mauvais, J., Sanders, C., Ward, R.T., and Webber, P. (1995). Transgenic canola and soybean seeds with increased lysine. Biotechnology (N. Y.) **13:** 577–582.

Frerman, F.E. (1988). Acyl-CoA dehydrogenases, electron transfer flavoprotein and electron transfer flavoprotein dehydrogenase. Biochem. Soc. Trans. **16:** 416–418.

Frerman, F.E., and Goodman, S.I. (2001). Defects of electron transfer flavoprotein and electron transfer flavoprotein-ubiquinone oxidoreductase: Glutaric acidemia type II. In The Metabolic and Molecular Bases of Inherited Disease, C.R. Scriver, W.S. Sly, B. Childs, A.L. Beaudet, and D. Valle, eds (New York: McGraw-Hill), pp. 2357–2365.

Frizzi, A., Huang, S., Gilbertson, L.A., Armstrong, T.A., Luethy, M.H., and Malvar, T.M. (2008). Modifying lysine biosynthesis and catabolism in corn with a single bifunctional expression/silencing transgene cassette. Plant Biotechnol. J. **6:** 13–21.

Galili, G., Tang, G., Zhu, X., and Gakiere, B. (2001). Lysine catabolism: A stress and development super-regulated metabolic pathway. Curr. Opin. Plant Biol. **4:** 261–266.

Ghadimi, H., Chou, W.S., and Kesner, L. (1971). Biosynthesis of saccharopine and pipecolic acid from L- and DL-14C-lysine by human and dog liver in vitro. Biochem. Med. **5:** 56–66.

Gu, L., Jones, A.D., and Last, R.L. (2010). Broad connections in the Arabidopsis seed metabolic network revealed by metabolite profiling of an amino acid catabolism mutant. Plant J. **61:** 579–590.

Heazlewood, J.L., Tonti-Filippini, J.S., Gout, A.M., Day, D.A., Whelan, J., and Millar, A.H. (2004). Experimental analysis of the Arabidopsis mitochondrial proteome highlights signaling and regulatory components, provides assessment of targeting prediction programs, and indicates plant-specific mitochondrial proteins. Plant Cell **16:** 241–256.

Hörtensteiner, S. (2006). Chlorophyll degradation during senescence. Annu. Rev. Plant Biol. **57:** 55–77.

Houmard, N.M., Mainville, J.L., Bonin, C.P., Huang, S., Luethy, M.H., and Malvar, T.M. (2007). High-lysine corn generated by endosperm-specific suppression of lysine catabolism using RNAi. Plant Biotechnol. J. **5:** 605–614.

Ishizaki, K., Larson, T.R., Schauer, N., Fernie, A.R., Graham, I.A., and Leaver, C.J. (2005). The critical role of Arabidopsis electron-transfer flavoprotein:ubiquinone oxidoreductase during dark-induced starvation. Plant Cell **17:** 2587–2600.

Ishizaki, K., Schauer, N., Larson, T.R., Graham, I.A., Fernie, A.R., and Leaver, C.J. (2006). The mitochondrial electron transfer flavoprotein complex is essential for survival of Arabidopsis in extended darkness. Plant J. **47:** 751–760.

Karimi, M., Inzé, D., and Depicker, A. (2002). GATEWAY vectors for Agrobacterium-mediated plant transformation. Trends Plant Sci. **7:** 193–195.

Kopka, J., et al. (2005). GMD@CSB.DB: The Golm Metabolome Database. Bioinformatics **21:** 1635–1638.

Kunz, H.H., Scharnewski, M., Feussner, K., Feussner, I., Flugge, U.I., Fulda, M., and Gierth, M. (2009). The ABC transporter PXA1 and peroxisomal β-oxidation are vital for metabolism in mature leaves of Arabidopsis during extended darkness. Plant Cell **21:** 2733–2749.

Larson, T.R., and Graham, I.A. (2001). Technical advance: A novel technique for the sensitive quantification of acyl CoA esters from plant tissues. Plant J. **25:** 115–125.

Lehmann, M., Schwarzlander, M., Obata, T., Sirikantaramas, A., Burow, M., Olsen, C., Tohge, T., Fricker, M., Moller, B., Fernie, A., Sweetlove, L.J., and Laxa, M. (2009). The metabolic response of Arabidopsis roots to oxidative stress is distinct from that of heterotrophic cells in culture and highlights a complex relationship between the levels of transcripts, metabolites, and flux. Mol. Plant **2:** 390–406.

Lim, P.O., Kim, H.J., and Nam, H.G. (2007). Leaf senescence. Annu. Rev. Plant Biol. **58:** 115–136.

Lisec, J., Schauer, N., Kopka, J., Willmitzer, L., and Fernie, A.R. (2006). Gas chromatography mass spectrometry-based metabolite profiling in plants. Nat. Protoc. **1:** 387–396.

Luedemann, A., Strassburg, K., Erban, A., and Kopka, J. (2008). TagFinder for the quantitative analysis of gas chromatography-mass

spectrometry (GC-MS)-based metabolite profiling experiments. Bioinformatics **24:** 732–737.

Mills, P.B., Struys, E., Jakobs, C., Plecko, B., Baxter, P., Baumgartner, M., Willemsen, M.A., Omran, H., Tacke, U., Uhlenberg, B., Weschke, B., and Clayton, P.T. (2006). Mutations in antiquitin in individuals with pyridoxine-dependent seizures. Nat. Med. **12:** 307–309.

O'Connor, G., King, M., Salomons, G., Jakobs, C., King, M., and Salomons, G. (2009). A novel mutation as a cause of L-2-hydroxyglutaric aciduria. J. Neurol. **256:** 672–673.

Oh, S.A., Lee, S.Y., Chung, I.K., Lee, C.H., and Nam, H.G. (1996). A senescence-associated gene of Arabidopsis thaliana is distinctively regulated during natural and artificially induced leaf senescence. Plant Mol. Biol. **30:** 739–754.

Porra, R.J., Thompson, W.A., and Kriedemann, P.E. (1989). Determination of accurate extinction coefficients and simultaneous equations for assaying chlorophylls a and b extracted with four different solvents: Verification of the concentration of chlorophyll standards by atomic absorption spectroscopy. Biochim. Biophys. Acta **975:** 384–394.

Pružinská, A., Tanner, G., Aubry, S., Anders, I., Moser, S., Müller, T., Ongania, K.-H., Kräutler, B., Youn, J.-Y., Liljegren, S.J., and Hörtensteiner, S. (2005). Chlorophyll breakdown in senescent Arabidopsis leaves: Characterization of chlorophyll catabolic enzymes involved in the degreening reaction. Plant Physiol. **139:** 52–63.

Rasmusson, A.G., Geisler, D.A., and Moller, I.M. (2008). The multiplicity of dehydrogenases in the electron transport chain of plant mitochondria. Mitochondrion **8:** 47–60.

Reyes, A.R., Bonin, C.P., Houmard, N.M., Huang, S., and Malvar, T.M. (2009). Genetic manipulation of lysine catabolism in maize kernels. Plant Mol Biol **69:** 81–89.

Roessner, U., Luedemann, A., Brust, D., Fiehn, O., Linke, T., Willmitzer, L., and Fernie, A.R. (2001). Metabolic profiling allows comprehensive phenotyping of genetically or environmentally modified plant systems. Plant Cell **13:** 11–29.

Roessner-Tunali, U., Hegemann, B., Lytovchenko, A., Carrari, F., Bruedigam, C., Granot, D., and Fernie, A.R. (2003). Metabolic profiling of transgenic tomato plants overexpressing hexokinase reveals that the influence of hexose phosphorylation diminishes during fruit development. Plant Physiol. **133:** 84–99.

Roessner-Tunali, U., Liu, J., Leisse, A., Balbo, I., Perez-Melis, A., Willmitzer, L., and Fernie, A.R. (2004). Kinetics of labelling of organic and amino acids in potato tubers by gas-chromatography mass-spectrometry following incubation in ^{13}C labelled isotopes. Plant J. **39:** 669–679.

Ruzicka, F.J., and Beinert, H. (1977). A new iron-sulfur flavoprotein of the respiratory chain. A component of the fatty acid beta oxidation pathway. J. Biol. Chem. **252:** 8440–8445.

Schauer, N., Steinhauser, D., Strelkov, S., Schomburg, D., Allison, G., Moritz, T., Lundgren, K., Roessner-Tunali, U., Forbes, M.G., Willmitzer, L., Fernie, A.R., and Kopka, J. (2005). GC-MS libraries for the rapid identification of metabolites in complex biological samples. FEBS Lett. **579:** 1332–1337.

Schelbert, S., Aubry, S., Burla, B., Agne, B., Kessler, F., Krupinska, K., and Hörtensteiner, S. (2009). Pheophytin pheophorbide hydrolase (pheophytinase) is involved in chlorophyll breakdown during leaf senescence in Arabidopsis. Plant Cell **21:** 767–785.

Sienkiewicz-Porzucek, A., Sulpice, R., Osorio, S., Krahnert, I., Leisse, A., Urbanczyk-Wochniak, E., Hodges, M., Fernie, A.R., and Nunes-Nesi, A. (2010). Mild reductions in mitochondrial NAD-dependent isocitrate dehydrogenase activity result in altered nitrate assimilation and pigmentation but do not impact growth. Mol. Plant **3:** 156–173.

Sodek, L., and Wilson, C.M. (1970). Incorporation of leucine C14 and lysine into protein in the developing endosperm of normal and *opaque-2* corn. Arch. Biochem. Biophys. **140:** 29–38.

Stepansky, A., Less, H., Angelovici, R., Aharon, R., Zhu, X., and Galili, G. (2006). Lysine catabolism, an effective versatile regulator of lysine level in plants. Amino Acids **30:** 121–125.

Struys, E.A., and Jakobs, C. (2010). Metabolism of lysine in a-amino-adipic semialdehyde dehydrogenase-deficient fibroblasts: Evidence for an alternative pathway of pipecolic acid formation. FEBS Lett. **584:** 181–186.

Struys, E.A., Salomons, G.S., Achouri, Y., van Schaftingen, E., Grosso, S., Craigen, W.J., Verhoeven, N.M., and Jakobs, C. (2005). Mutations in the D-2-hydroxyglutarate dehydrogenase gene cause D-2-hydroxyglutaric aciduria. Am. J. Hum. Genet. **76:** 358–360.

Studart-Guimarães, C., Fait, A., Nunes-Nesi, A., Carrari, F., Usadel, B., and Fernie, A.R. (2007). Reduced expression of the succinyl-coenzyme A ligase can be compensated for by up-regulation of the gamma-aminobutyrate shunt in illuminated tomato leaves. Plant Physiol. **145:** 626–639.

Swanson, M.A., Usselman, R.J., Frerman, F.E., Eaton, G.R., and Eaton, S.S. (2008). The iron-sulfur cluster of electron transfer flavoprotein-ubiquinone oxidoreductase is the electron acceptor for electron transfer flavoprotein. Biochemistry **47:** 8894–8901.

Tieman, D., Taylor, M., Schauer, N., Fernie, A.R., Hanson, A.D., and Klee, H.J. (2006). Tomato aromatic amino acid decarboxylases participate in synthesis of the flavor volatiles 2-phenylethanol and 2-phenylacetaldehyde. Proc. Natl. Acad. Sci. USA **103:** 8287–8292.

Timm, S., Nunes-Nesi, A., Parnik, T., Morgenthal, K., Wienkoop, S., Keerberg, O., Weckwerth, W., Kleczkowski, L.A., Fernie, A.R., and Bauwe, H. (2008). A cytosolic pathway for the conversion of hydroxy-pyruvate to glycerate during photorespiration in *Arabidopsis*. Plant Cell **20:** 2848–2859.

Tohge, T., and Fernie, A.R. (2010). Combining genetic diversity, informatics, and metabolomics to facilitate annotation of plant gene function. Nat. Protoc. **5:** 1210–1227.

Ufaz, S., and Galili, G. (2008). Improving the content of essential amino acids in crop plants: goals and opportunities. Plant Physiol. **147:** 954–961.

Usadel, B., Obayashi, T., Mutwil, M., Giorgi, F.M., Bassel, G.W., Tanimoto, M., Chow, A., Steinhauser, D., Perrsson, S., and Provart, N.J. (2009). Co-expression tools for plant biology: Opportunities for hypothesis generation and caveats. Plant Cell Environ. **32:** 1633–1651.

Zhang, J., Frerman, F.E., and Kim, J.J. (2006). Structure of electron transfer flavoprotein-ubiquinone oxidoreductase and electron transfer to the mitochondrial ubiquinone pool. Proc. Natl. Acad. Sci. USA **103:** 16212–16217.

Zhu, X., and Galili, G. (2003). Increased lysine synthesis coupled with a knockout of its catabolism synergistically boosts lysine content and also transregulates the metabolism of other amino acids in *Arabidopsis* seeds. Plant Cell **15:** 845–853.

Zinnanti, W.J., Lazovic, J., Housman, C., LaNoue, K., O'Callaghan, J.P., Simpson, I., Woontner, M., Goodman, S.I., Connor, J.R., Jacobs, R.E., and Cheng, K.C. (2007). Mechanism of age-dependent susceptibility and novel treatment strategy in glutaric acidemia type I. J. Clin. Invest. **117:** 3258–3270.

Identification of the 2-Hydroxyglutarate and Isovaleryl-CoA Dehydrogenases as Alternative Electron Donors Linking Lysine Catabolism to the Electron Transport Chain of *Arabidopsis* Mitochondria

Wagner L. Araújo, Kimitsune Ishizaki, Adriano Nunes-Nesi, Tony R. Larson, Takayuki Tohge, Ina Krahnert, Sandra Witt, Toshihiro Obata, Nicolas Schauer, Ian A. Graham, Christopher J. Leaver and Alisdair R. Fernie

This information is current as of March 28, 2012